INTERNATIONAL JOURNAL OF
COASTAL, OFFSHORE & ENVIRONMENTAL ENGINEERING IJCOE Vol.8/No. 2/Spring 2023 (40-47)

Available online at: www. Ijcoe.org

Study of surface fluxes over the Northern Indian Ocean Seas

Rozana Ghandy[1], AbbasAli Aliakbari Bidokhti[2*], Parviz Irannejad[3], Mojtaba Ezam[4]

[1] *Faculty of Natural Resources and Environment, Science and Research Branch, Islamic Azad University, Tehran, Iran*

[2*] *Prof. of Environmental Fluid Mechanics Institute of Geophysics University of Tehran, Tehran, Iran; bidokhti@ut.ac.ir*

[3] *Institute of Geophysics University of Tehran, Tehran, Iran*

[4] *Faculty of Natural Resources and Environment, Science and Research Branch, Islamic Azad University, Tehran, Iran*

ARTICLE INFO

Article History:
Received: 07 Aug. 2021
Accepted: 23 May. 2023

Keywords:
Latent heat flux
Sensible heat flux
Persian Gulf
Gulf of Oman
Northern Indian Ocean

ABSTRACT

The open waters of the north Indian Ocean (NIO), which itself includes the Persian Gulf (PG), the Gulf of Oman (GO), and the Arabian Sea (AS), are subject to different meteorological forcing that can affect surface fluxes of these environments. In this study, latent heat flux (Q_{LH}), sensible heat flux (Q_{SH}), and surface wind stress (τ) between these regions are investigated. The reanalysis data from the data sets of the National Centers for Environmental Prediction (NCEP) and the European Center for Medium-Range Weather Forecasts (ECMWF) for these three regions for 14 years (2013-2000) are used. The results are compared with the measured data in the GO that show ECMWF reanalysis data are more consistent with the measured data in this period. We compare the average monthly, seasonal and annual values of Q_{LH}, Q_{SH} and τ of the PG, GO, and AS. The annual averages of Q_{LH} for the PG, the GO, and the AS are -128.63, -118.76, and -118.03 (Wm^{-2}) and the annual averages of Q_{SH} are -1.28, -3.88, and -5.67 (Wm^{-2}) respectively. The annual averages of τ are 0.074, 0.075, 0.036 (Pa) for these areas respectively. Also the annual average SST is 27, 26.56, and 27.14 (ºC) respectively for these areas. Based on the results, different regimes of the PG wind and its dust storms, on the one hand, and the limited and semi-closed space of the PG with its shallow depth, on the other hand, leads to different behaviors of Q_{LH} and Q_{SH} in PG area, in comparison with the other two environments (namely GO and AS).

1. Introduction

Study of the distribution of heat fluxes (*Qs*) between air and sea has an influential role in understanding changes in weather systems, climate conditions, and changes in water surface temperature and transfer of gases across the air-sea interface [1].

The heat storage capacity of the oceans large and is mainly provided at interface [2]. Wind stress and heat exchange at the interface between air and sea can cause turbulent mixing of the water mass and determine the ocean mixed layer [3]. The warming process in the Indian Ocean is a major contributor to the overall average sea surface temperature (SST) trend that can have a global atmospheric effect especially in the tropical Indian Ocean. The Arabian Sea (AS) in the face of seasonal atmospheric forcing undergoes many changes, which are mainly annual changes and some interannual intermediate [4].

The net heat transfer in the earth system is mainly mediated by solar radiation (Q_{SW}), longwave radiation (Q_{LW}), sensible heat flux (Q_{SH}), convection (Q_V) and latent heat flux (Q_{LH}) [5]; according to the following formula:

$$Q=Q_{SW}+Q_{LW}+Q_{LH}+Q_{SH}+Q_V \quad (1)$$

Due to the importance of ocean *Q* distribution, many studies have been performed to identify each of the parameters in different oceans and seas [6]. Each of the parameters can be calculated directly (by direct measurement) or indirectly (using empirical formulas).

Because direct measurements are costly and limited in time and domain [5], the use of empirical formulas as aerodynamic bulk formula are commonly used to calculate Q_{SH} and Q_{LH}, which are as follows:

$$Q_{SH}=\rho\, C_p\, C_S\, U_{10}\,(t_s- t_a) \quad (2)$$

$$Q_{LH}=\rho\, L_e\, C_L\, U_{10}\,(q_s- q_a) \quad (3)$$

where ρ air is density, L_e is the latent heat of vaporization, C_p is the specific heat capacity of air at constant pressure, C_L and C_S are latent and perceptible heat transfer coefficients, U_{10} is the wind speed at 10 m above sea level, t_s and t_a are respectively air temperature near the sea level and temperature at 10 meters above sea level, q_s and q_a are the specific humidity of the air just above sea level and the specific humidity of the air at 10 meters above sea level, respectively. Equations 2 and 3 have been often used in previous studies with more appropriate estimates of transfer coefficients [7, 8, 9, 10, 11, 12].

Due to the availability of essential information for calculating two important parameters Q_{SH} and Q_{LH}, analyzing these two parameters and comparing them between several oceans (or seas) are key findings in determining changes in weather and climatic conditions. These two parameters also play essential roles in atmospheric and sea coupling models, which can effectively determine climate change [1, 5, 13]. It should be noted that Q_{LH} values over the ocean are significantly higher than Q_{SH} values [5].

One of the critical areas for studying heat flux distribution is the northern Indian Ocean (NIO), which is affected by climate change and is widely included in the Arabian Sea (AS), Gulf of Oman (GO), and Persian Gulf (PG). Any change of these environments can change the climate of the surrounding areas.

The study area and its coordinate are shown in Figure.1 and Table 1 respectively. Study of surface fluxes distributions are important in the NIO because of the special and unique conditions of this region. Due to the fact that this area is located in a hot and dry region and is mainly enclosed between lands. Some previous study has shown a heat loss by Q_{LH} up to about 671 (Wm^{-2}) due to the occurrence of dry winds that could also cause a significant amount of dust in the atmosphere [14, 15]. The 35 years of wind rose showed in several locations of the NIO for 35 years are shown in Figure. 1 (references of this data are ECMWF-ERA5)[1].

The Shamal wind is the most energetic wind in the Persian Gulf region. It is a strong northerly to the northwesterly wind that blows along the axis of the Persian Gulf in both winter and summer. The winter Shamal winds occur mainly from November through March, while the summer Shamal winds with much less important in terms of wind strength, accompanying weather conditions and that are generally persistent from May to early July. Moreover, south to southeasterly Kaus winds often blows which are considered local winds [15,16]. Also, the prevailing wind direction of the GO and the AS is (following Figure. 1) from the west and southwest which is significant different from the wind regime in the PG. In addition, the mean rate of evaporation in these areas is reported up to be about 5 meters per year [17, 18].

Table 1. Coordinates of the study area

	Long(°)	Lat(°)
NIO	48-74	10-31
PG	48-56	24-31
GO	56-60	22-27
AS	51-74	10-22

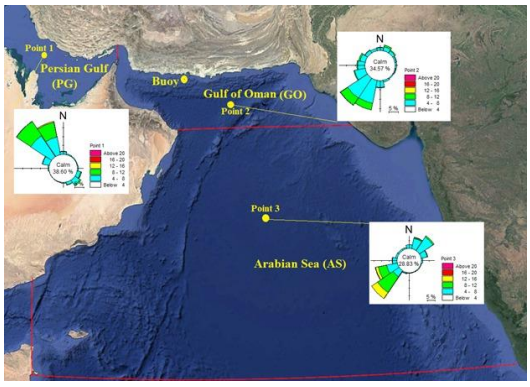

Figure 1. Some windroses in the study area (ECMWF- ERA5) and location of meteorological measurement data in PG.

The wind speed and direction affect climate conditions directly and indirectly. The results showed that the wind direction slightly affects evaporation, but the wind speed can significantly change the rate of evaporation in the PG [19] as the environment is dry. Climate change affects the wind field and the wind mostly produces sea waves [20]. Hence evaluating the wind field is important for calculating surface heat fluxes.

[1] ECMWF Reanalysis 5th Generation

As seen in Eq. 2 and 3, Q_{SH} and Q_{LH} depend on U_{10} directly and indirectly, as the wind can significantly affect the temperature and humidity values, and consequently, they influence the Q_{SH} and Q_{LH} indirectly. Therefore, the relationship between the wind and Q distribution is one of the most important issues in climate impact determination [13, 21, 22]. The effect of wind, which is studied as the effective parameter for surface wind stress (τ), is calculated as follows:

$$\tau = \rho\, C_D\, (U_{10})^2 \qquad (4)$$

where C_D is the drag coefficient which is somehow depends on wind speed. In this paper, using meteorological data and bulk experimental formula, the values of Q_{SH} and Q_{LH}, and τ for the three parts of the AS, GO, and PG, which have not been discussed separately before (As far as the authors know), have been calculated and compared for the three reigns. For this purpose, ECMWF [2] and NCEP [3] meteorological reanalysis data are used in this study. First, these data are validated by measurement data in a GO location which is shown in Figure 1, and then more appropriate data set has been selected for further analysis.

2. Datasets and Method

The more appropriate estimation of heat flux leads to more accurate results in the climate study. Therefore, the quality of ECMWF and NCEP meteorological data should be evaluated. In this study, a meteorological measurement station in the GO (Figure. 1) is applied to estimate the Q values. This data is used to evaluate the ECMWF and NCEP reanalysis data in NIO. The average monthly values of Q_{SH}, Q_{LH}, and τ are calculated based on measurement and reanalysis of meteorological data at the buoy location (point 2, for 2013). Figure. 2 (a) and (b) show respectively the comparison of monthly mean values of Q_{LH} and Q_{SH} calculated by Buoy, ECMWF, and NCEP meteorological data. It should be noted that the positive values in this paper represent heat transfer from air to water and the negative values indicate heat transfer from water to air. According to this graph, Q_{LH} values from ECMWF reanalysis and buoy data are significantly higher than Q_{SH} values. As seen from the buoy values, the maximum value of Q_{LH} is about -450 (Wm^{-2}), which occurs in July. In the same month, the amount of Q_{SH} is about +30 (Wm^{-2}). In fact, positive buoy Q_{SH} is associated with the exchange of heat from the air to water.

Figure. 2 (c) shows the comparison of monthly mean values of τ calculated by Buoy, ECMWF, and NCEP meteorological data. The value of τ was the highest in July (about 0.04 Pa), and the average values of τ are about 0.02 Pa. Table 2 also shows the average annual values of Q_{SH}, Q_{LH}, and τ. As seen in this table, the annual average of Q_{LH}, Q_{SH}, and τ are about 276 (Wm^{-2}), 19.8 (Wm^{-2}), and 0.03 (Pa), respectively. In this study, the monthly mean values of Q_{SH}, Q_{LH}, and τ are also calculated based on the ECMWF and NCEP meteorological data at the buoy location for 2013, and their variation are plotted in Figure.2. According to the results, it is clear that the ECMWF reanalysis data is more consistent with the Buoy data and its evident for all three parameters Q_{SH}, Q_{LH}, and τ. The error index of ECMWF reanalysis data for calculating Q_{SH}, Q_{LH}, and τ are about 30, 2, and 60%, respectively. However, the error-index of acquired NCEP reanalysis data is about 99, 9, and 120%, respectively. Based on the error-index, it is clear that the ECMWF reanalysis data in the buoy location is more accurate than the NCEP acquired reanalysis data. Therefore, ECMWF reanalysis data (with a resolution of 0.25 degrees) is used to calculate Q_{SH}, Q_{LH}, and τ in the whole study area.

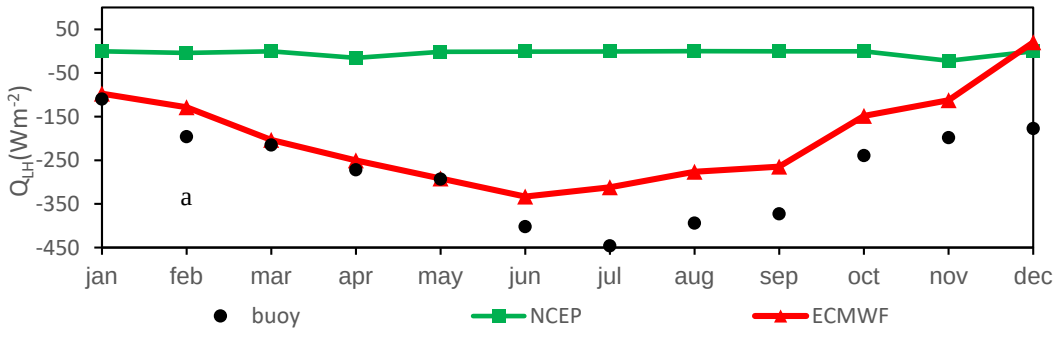

[2] European Center Medium-Range Weather Forecasts

[3] National Center for Environmental Prediction Final

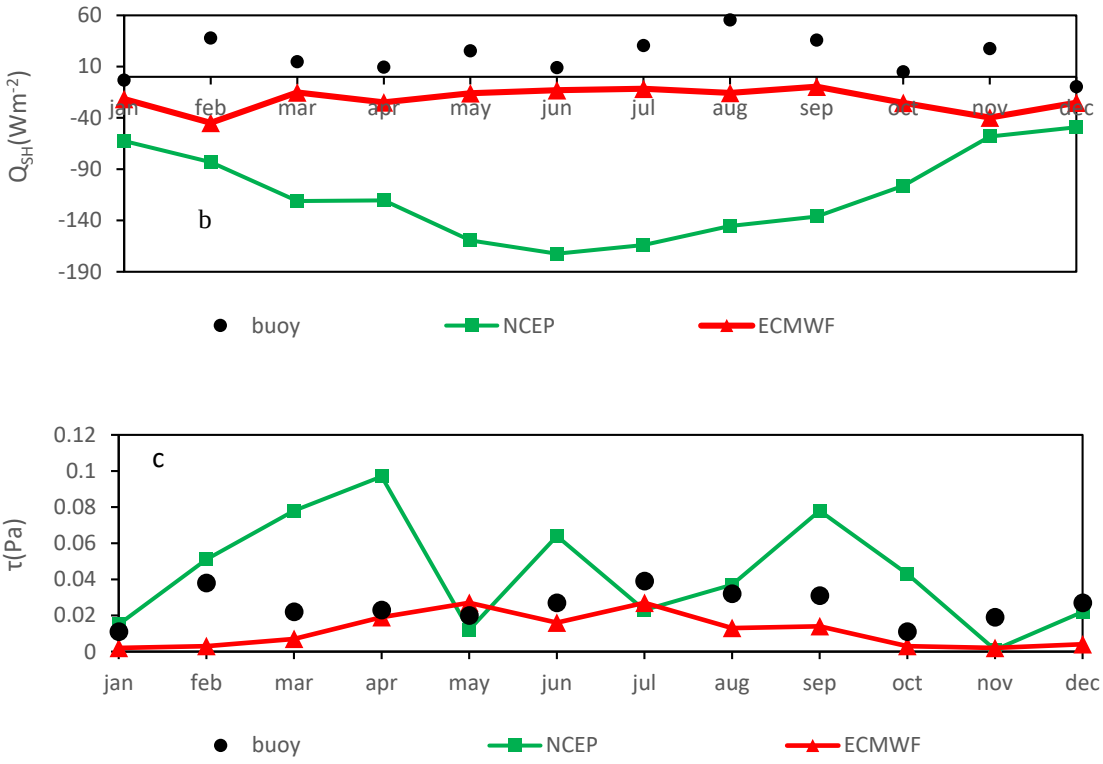

Figure 2. Monthly mean of Q_{LH} (a), Q_{SH} (b), and τ (c) at buoy location in 2013

Table 2. Monthly mean of Q_{LH}, Q_{SH} (in Wm^{-2}), and τ (in Pa) at the measurement location for 2013

	ECMWF			NCEP			Measurement		
	Q_{LH}	Q_{SH}	τ	Q_{LH}	Q_{SH}	τ	Q_{LH}	Q_{SH}	τ
Mean	-199.8	-21.9	0.01	-42.18	-77.7	0.04	-276.4	19.8	0.03

3. Results and Discussion

In this study, 14-year ECMWF reanalysis data were used to calculate the values of Q_{LH} and Q_{SH}, and τ for the NIO and separately for the AS, GO, and PG regions. The values were calculated and compared monthly (average per month over 14 years), seasonal average (average per season over 14 years), and the annual average for AS, GO, and the PG regions.

3.1. Monthly Variability

Figure. 3 shows the monthly mean values of Q_{LH} over the study period for AS, GO, and the PG regions. As shown in this Figure, the minimum, maximum, and average Q_{LH} parameter changes for each month are shown as Box and Whisker diagrams during the study period. The values of Q_{LH} show heat exchange from the sea to the atmosphere. The highest amount of Q_{LH} was recorded in December and January when it was about 200 (Wm^{-2}) in the PG. Also, the minimum value of this parameter is about 60 (Wm^{-2}), which occurs in August and September in the GO. The trend of Q_{LH} variation is the same for the three regions of the AS, GO, and the PG; the amount of Q_{LH} decreases from December to April and then increases from April to June. Then, the amount of Q_{LH} decreases until September, and finally, Q_{LH} increases until December. These changes are the same for the three regions. It is observed that Q_{LH} in the PG is higher than those of the GO, and the GO values are higher than those of the AS from January to June. This pattern has been observed irregularly for other months, with Q_{LH} in the GO being lower than those of the PG and the AS in July, August, and September.

Figure. 4 shows monthly mean values of Q_{SH} over the study period. The results show that heat transfer is from the sea to the atmosphere in the AS. For the PG and GO, Q_{SH} transfers from the atmosphere to the sea in

June, July, August, and September; in other months, heat transfer via Q_{SH} is from the sea to the atmosphere. In other words, the transfer of Q_{SH} between the sea and the atmosphere for the AS in the four months of June, July, August, and September is different from the PG and GO. The range of Q_{SH} with a range of -20 to +20 for the NIO is much lower than those of the Q_{LH} values. It is also observed that the slope of Q_{SH} changes from December to July, which is increasing, that is different from the slope of Q_{SH} changes from July to December, which is decreasing.

Figure 5 shows the monthly mean values of τ over the study period. The trend of τ variation is the same as Q_{SH} at NIO, and it seems that there is a strong correlation between these two parameters. Moreover, the changes of τ in the AS are different from those of the PG and the GO in the four months of June, July, August, and September. In other words, τ in the AS is less than those of the PG and the GO in these four months.

In this section, the monthly average of Q_{LH} and Q_{SH}, and τ in three AS, GO, and PG regions have been studied. Examination of the results shows that the trend of monthly changes in Q_{SH}, τ is quite similar. A strong correlation has been observed between the studied parameters in the NIO. As the τ increases, the amount of Q_{LH} decreases; this means that heat transfer from sea to air through Q_{LH} is reduced in summer compared to winter. The heat exchange from the sea to the atmosphere changes through the Q_{SH} in summer with the increase in τ; in this way, Q_{SH} is transferred from the atmosphere to the sea in summer and is from the sea to the atmosphere in winter.

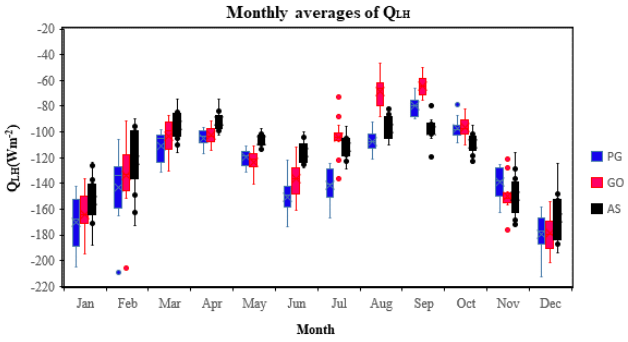

Figure 3. Monthly mean of Q_{LH} in the study period of the AS, GO, and PG

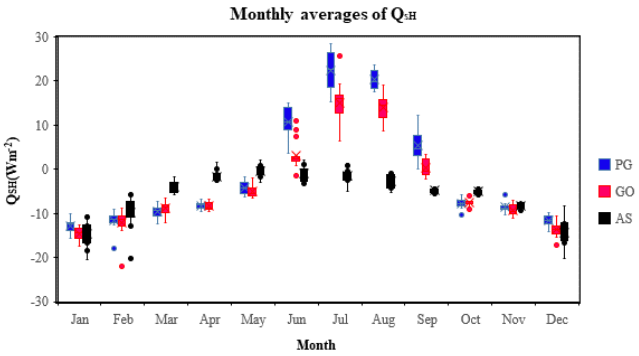

Figure 4. Monthly mean of Q_{SH} in the study period of the AS, GO, and PG

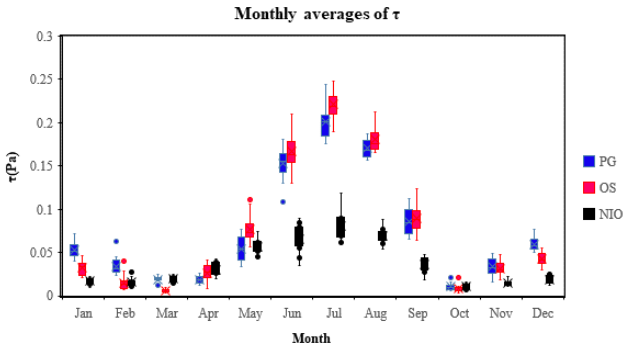

Figure 5. Monthly mean of τ in the study period of the AS, GO, and PG

3.2. Seasonal Variability

Figure 6 shows the seasonal mean Q_{LH} values over the study period. As shown in this Figure, the minimum, maximum, and mean values of the Q_{LH} changes for each season. The seasonal study of Q_{LH} shows that the average Q_{LH} varies in different seasons and the heat transfer is from the sea to the atmosphere by this means. The highest amount of Q_{LH} was recorded in the fall, which was about 150 (Wm^{-2}). Also, the minimum value of this parameter is about 80 (Wm^{-2}), which occurs in winter in the GO. According to Figure. 6, heat transfer from the sea to the atmosphere in the form of Q_{LH} is in winter and spring in the PG has been more than those of the GO and the GO, which is still more than that of the AS. In summer, heat transfer from the sea to the atmosphere via Q_{LH} is observed in the PG more than the AS, and in the AS it is more than that of the GO. Also, the amount of Q_{LH} in autumn is almost the same for the three studied areas.

Figure. 7 shows the seasonal mean values of Q_{SH} during the study period. The seasonal review of Q_{SH} shows that the mean Q_{SH} varies seasonally, similar to what is discussed in the monthly changes. Heat transfer through the Q_{SH} in the AS has always been from the sea to the atmosphere. On the other hand, for the PG and

the GO, heat transfer through the Q_{SH} has been from the atmosphere to the sea in the summer.

Figure. 8 shows the seasonal mean values of τ over the study period. In general, τ values in the PG and the GO are higher than that in the AS. In summer, stronger winds are observed in both the PG and the GO. This could be the reason for Q_{SH} summer heat transfer which is from the atmosphere to the sea. For the other three seasons, the heat transfer is Q_{SH} from the sea to the atmosphere. Increase in wind stress also affects the intensity of Q_{LH}. In fact, with increasing wind stress in summer, the value of Q_{LH} also decreases, may be to the waves breaking sheltering effect that can reduce the surface evaporation coefficient at stronger winds.

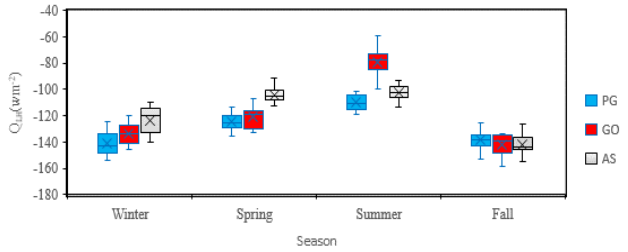

Figure 6. Seasonal mean Q_{LH} in the study period of the AS, GO, and PG

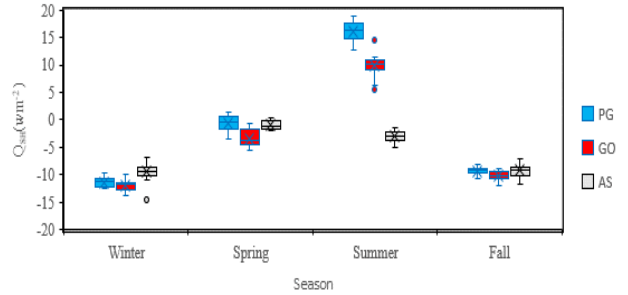

Figure 7. Seasonal mean Q_{SH} in the study period of the AS, GO, and PG

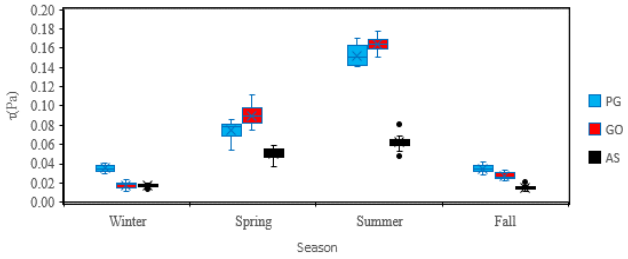

Figure 8. Seasonal mean τ in the study period of the AS, GO, and PG

3.3. Annual Variability

Figure. 9 shows the annual mean Q_{LH} values over the study period. As shown in Figure. 9, the annual average Q_{LH} in the PG is higher than the GO and the AS. The Q_{LH} transfer from the sea to the atmosphere in the PG is more than those of the two basins of the GO and the AS, which can be due to the almost being semi-closed environment of the PG with shallow depth, compared to the GO and the AS, which provides more heat transfer to the atmosphere in the shallow PG area. Of course, higher wind speeds in PG relative to those of the GO and the AS are also influential. Since the PG air is desert and dry [1], the wind brings dry air to the PG and reduces humidity. Decreased humidity leads to more evaporative heat transfer from the sea to the atmosphere.

Figure. 10 shows the average annual Q_{SH} values over the study period. As shown in Figure. 10, in all years, the annual average Q_{SH} in the PG is lower than that of the GO, and in the GO it is still lower than that of the AS, which can be due to strong winds in the PG and to s0ome extent, in the GO.

Figure. 11 shows the annual mean values of τ over the study period. In general, τ values in the PG and the GO are higher than that in the AS. The mean value of τ recorded in the PG and the GO are almost twice that of the AS. Furthermore, τ combined with specific PG conditions (shallow depths and semi-closed space) has created unique climate conditions in the NIO area.

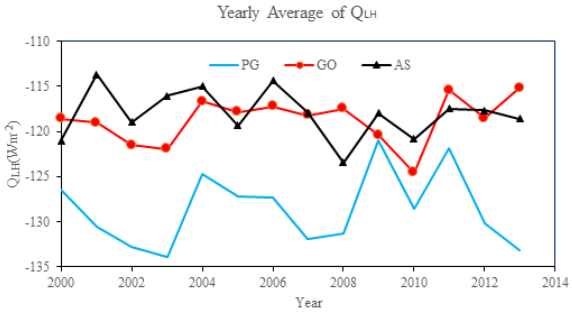

Figure 9. Annual mean Q_{LH} in the study period of the AS, GO, and PG

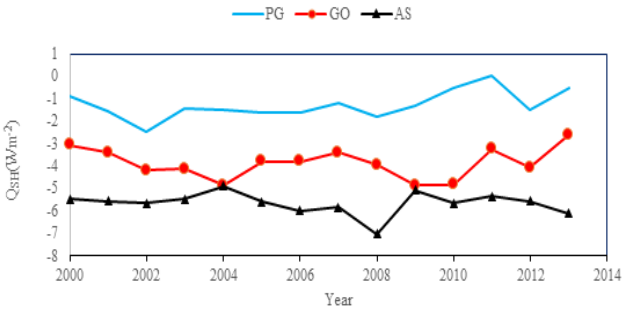

Figure 10. Annual mean Q_{SH} in the study period of the AS, GO, and PG

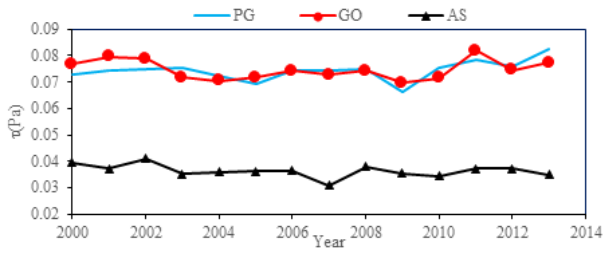

Figure 11. Annual mean τ in the study period of the AS, GO, and PG

4. Conclusions

This paper investigates the value of two crucial heat transfer parameters between the sea surface and the atmosphere, namely Q_{LH}, and Q_{SH}, in the NIO area. For a more detailed study, this region has been divided into three sub-regions: the PG, GO and AS. The values of Q_{LH} and Q_{SH} have been calculated and compared with the help bulk transfer formula on a monthly, seasonal and annual averages in these three regions. In order to calculate the mentioned fluxes, meteorological parameters such as wind speed, air humidity difference between climate levels, and temperature difference between climate levels are used. Observational measurements were used along with NCEP reanalysis data, leading to the following concluding points:

• Surface mean annual wind stress in the PG and the GO are usually higher than that in the AS.

• Considering that the τ in the PG and to some extent, in the GO are higher than that of the AS, and on the other hand, since the PG air is usually desert and dry, the wind brings the dry air to the PG and reduces the humidity. Hence, decreased humidity leads to more Q_{LH} transfer in PG from the sea to the atmosphere is larger than those in the AS and the GO.

• In winter, heat transfer from the sea to the atmosphere via Q_{LH} in the PG has been more than that of the GO and the GO values are more than that of the AS. In spring, heat transfer is mainly via Q_{LH} from the sea to the atmosphere in the PG and in the GO, and are almost "similar" and more than that of the AS. In summer, heat transfer from the sea to the atmosphere via Q_{LH} in the PG is also more than that of the AS, and that of the AS and is more than that of the GO.

• The Q_{SH} in the AS has always been from the sea to the atmosphere, but the PG and the GO in summer it has been from the atmosphere to the sea. Strong winds could be the reason for Q_{SH} summer heat transfer from the atmosphere to the sea. For the other three seasons, the heat transfer by Q_{SH} is from the sea to the atmosphere. Increased wind stress also affects the value of Q_{LH}. In fact, with increasing τ in summer, the intensity of Q_{LH} also decreases that may be due to sheltering effects of wind waves at stronger winds.

• Although it is difficult to fully understand the relationship between the parameters studied in this study, however, monsoonal and seasonal circulations in the area seem to determine the observed fluxes in the study area.

Acknowledgments

We acknowledge ECMW and NCEP for making available the data used in this study.

8. References

[1] Al Senafi, F., Anis, A. and Menezes, V. (2019). *Surface heat fluxes over the Northern Persian Gulf and the Northern Red Sea: evaluation of ECMWF-ERA5 and NASA-MERRA2 reanalyses*. Atmosphere,. 10(9): p. 504.

[2] Vissa, N.K., Satyanarayana, A.N.V. and Prasad Kumar, B. (2013). *Comparison of mixed layer depth and barrier layer thickness for the Indian Ocean using two different climatologies.* International J. of Climatology, 33(13), pp.2855-2870.

[3] Kara, A.B., Rochford, P.A. and Hurlburt, H.E., (2003). *Mixed layer depth variability over the global ocean*. Journal of Geophysical Research: Oceans, 108(C3).

[4] Mullah Esmailpour, S., Mehdizadeh, M., Hassanzadeh, E., Khalilabadi, M. (2018). *Determination of the depth of the mixed layer and investigation of the barrier layer during the summer and winter monsoon in the North Indian Ocean*. Hydrophysics, 3(2), pp.41-55

[5] Stewart, R. H. (2008) *Introduction to physical oceanography*, Robert H. Stewart.

[6] Cayan, D. R. (1992). *Latent and sensible heat flux anomalies over the northern oceans: Driving the sea surface temperature*. Journal of Physical Oceanography, 22(8), pp.859-881.

[7] Singh, R., Kishtawal, C.M., Pal, P.K. and Joshi, P.C. (2006). *Surface heat fluxes over global oceans exclusively from satellite observations*. Monthly weather review, 134, (3), pp.965-980.

[8] Banks, R.F., Bourassa, M .A., Hughes, P., O'Brien, J.J. and Smith, S.R. (2006). *January. Variability of surface turbulent fluxes over the Indian Ocean*. In 14th Conference on Interactions of the Sea and Atmosphere.

[9] Yu, L. and Weller, R.A. (2007). *Objectively analyzed air–sea heat fluxes for the global ice-free oceans (1981–2005)*. Bulletin of the American Meteorological Society, 88(4), pp.527-540.

[10] Yu, L., Weller, R.A. and Sun, B. (2004). *Improving latent and sensible heat flux estimates for the Atlantic Ocean (1988–99) by a synthesis approach*. Journal of Climate, 17(2), pp.373-393.

[11] Yu, L., Jin, X. and Weller, R.A. (2007). *Annual, seasonal, and interannual variability of air–sea heat fluxes in the Indian Ocean*. Journal of climate, 20(13), pp.3190-3209.

[12] Khademi, I., Akbarinasab, M., Bidokhti, A.A. and Khalilabadi, M.R. (2017). *Numerical calculation of Prandtl number in water column stratification in the Strait of Hormuz.* Journal of Marine Science and Technology, 16(3), pp.14-26.

[13] Ghose, S.K., Swain, D., Mathew, S. and Venkatesan, R. (2021). *Seasonal variability of air-sea fluxes in two contrasting basins of the North Indian Ocean*. Dynamics of Atmospheres and Oceans, 93, p.101183.

[14] Zolina, O., Dufour, A., Gulev, S.K. and Stenchikov, G. (2017). *Regional hydrological cycle over the Red Sea in ERA-Interim.* Journal of Hydrometeorology, 18(1), pp.65-83.

[15] Al Senafi, F. and Anis, A. (2015). *Shamals and climate variability in the Northern Persian Gulf from 1973 to 2012.* International Journal of climatology, 35(15): p. 4509-4528 .

[16] Rao, P.G., Hatwar, H.R., Al-Sulaiti, M.H. and Al-Mulla, A.H. (2003). *Summer shamals over the Persian Gulf*. Weather, 58(12), pp.471-478.

[17] Thoppil, P.G. and Hogan, P.J. (2010). *Persian Gulf response to a wintertime shamal wind event. Deep Sea Research Part I*: Oceanographic Research Papers, 57(8): p. 946-955 .

[18] Rezaei-Latifi, A. and Hosseinibalam, F. (2015). *An estimate of the surface heat fluxes transfer of the Persian Gulf with the overlying atmosphere.* Journal of Radiation Research and Applied Sciences, 8(3), pp.354-361.

[19] Mahpeykar, O. and Khalilabadi, M.R. (2021). *Numerical modelling the effect of wind on Water Level and Evaporation Rate in the Persian Gulf.* International Journal of coastal and offshore engineering, 6(1), pp.47-53.

[20] Pourali, M. and Kavianpour, M.R. (2023). Variation of monthly exploitable wave energy in the Gulf of Chabahar under a high-resolution CMIP6. International Journal Of Coastal, Offshore And Environmental Engineering, 8(1), pp.16-25.

[21] Tomita, H. and Kubota, M. (2004). Variability of surface heat flux over the Indian Ocean. Atmosphere-ocean, 42(3): p. 183-199.

[22] Shinoda, T., Hendon, H.H. and Glick, J. (1999). Intraseasonal surface fluxes in the tropical western Pacific and Indian Oceans from NCEP reanalysis. Monthly weather review, 127(5), pp.678-693.